Control of Porosity in SiO_2:PDMS Polycerams through Variations in Sol-Gel Processing and Polymer Content

T. Suratwala, K. Davidson, Z. Gardlund, and D.R. Uhlmann
Department of Materials Science and Engineering, Arizona Materials Laboratory
University of Arizona, 4715 E. Fort Lowell, Tucson, AZ 85712, USA

ABSTRACT

A series of optically transparent SiO_2: polydimethylsiloxane (PDMS) Polyceram monoliths have been synthesized by two-step acid/base sol-gel processes. Two different processing routes are discussed and compared; one synthetic route (Route 1) utilizes lower water content, shorter reflux times, and faster drying conditions compared to the other synthetic route (Route 2). The Route 1 Polycerams were all essentially non-porous at all PDMS contents examined (20-80 volume % PDMS). In contrast, the porosity of the Route 2 Polycerams varied dramatically as a function of PDMS content. The surface area and pore volume for a 0% PDMS Route 2 Polyceram were 573 m^2/gm and 0.59 cm^3/gm, respectively; the surface area and pore volume decreased with increasing PDMS content. The amount of porosity within the Polycerams is proposed to be controlled by the relative rates of condensation and evaporation during processing and by the amount of PDMS trapped in the pores. This ideas supported by the differences in the drying behavior with processing and by the structural information obtained by magic angle spinning solid-state ^{29}Si NMR of the Polyceram monoliths. Quantitative evaluation of the ^{29}Si NMR and porosity data are utilized to formulate structural models of these Polycerams. The structural models are then specifically used to describe the effect of porosity on the photostabilization of a laser dye doped within these Polyceram monoliths.

KEYWORDS: Porosity, Polydimethylsiloxane, Polycerams, Surface Area, MAS ^{29}Si NMR, N_2 adsorption BET, Pyrromethene 567, photostability

1. INTRODUCTION

Engineered porous materials are useful for a variety of important technologies including filters, absorbers, separation systems for gases, ions, small molecules and particles, low dielectric substrates, and thermal insulators[1]. Porous materials synthesized by sol-gel techniques represent an important class of engineered porous materials because of the ability to obtain a wide range of pore sizes and surface areas depending on the processing and composition. Sol-gel synthesized aerogels, xerogels, and porous vitrified silica have been extensively investigated for their porosities[2-5], while Polyceram materials, which are polymer-modified ceramic materials in which the organic and inorganic components are combined on a near-molecular scale, have only been recently studied[6-8].

A number of methods have been applied to control the porosity, surface area, and pore size distributions within sol-gel matrices. In a review by Brinker et. al.[3], these different techniques are discussed; a summary of these methods is illustrated in Table 1. One way to control the porosity is to manipulate the relative rates of condensation and solvent evaporation during sol-gel synthesis. When the condensation rate greatly exceeds the evaporation rate during drying, the material will tend to have a higher porosity. The high condensation rate increases the gel strength and limits the amount of shrinkage which takes place during drying. In contrast, when the evaporation rate exceeds the condensation rate, the material is more likely to shrink, resulting in a less porous material. A sol which is spin-coated to form a film is an example of the case where the evaporation rate is high with respect to the condensation rate. The condensation rate can be controlled by a number of factors such as the reactivity of the alkoxide, the pH of the solution, the catalyst, the nature and the amount of solvent present, and the H_2O:Si mole ratio. The evaporation rate can be controlled during drying by the solvent volatility, the drying temperature, the air flow, and the surface area of gel exposed to drying.

The effectiveness of varying the relative rates of condensation and evaporation for porosity control has been demonstrated with xerogels[3]; but to the authors' knowledge, this method has not been demonstrated with Polyceram materials. Non-porous materials have not been synthesized using this method with xerogels; only materials with decreased

SPIE Vol. 3136 • 0277-786X/97/$10.00

porosity have been achieved. With the incorporation of polymers or oligomers during synthesis, non-porous materials can be obtained. In the present study, we explore how porosity can be controlled within Polycerams by changes in the relative rates of condensation and evaporation during processing. The porosity and surface area are related to the processing conditions and polymer content, and structural models are developed based on NMR and BET data. Finally, the control of porosity and the structural model are utilized to obtain insight into the effects of porosity on the photostability of a laser dye doped within these SiO_2:PDMS Polycerams.

Table 1: Methods explored to control porosity in sol-gel matrices.

Method	Principle of Method	Comments
Particle Packing	•packing of colloidal particles creates pores which have sizes related to particle size	•uniform pore size obtained with uniform particle size •pore volume for spherical particles is always 33% regardless of particle size, assuming dense random packing
Aggregation of Fractals	•pores form through the aggregation of polymeric sols	•works only if clusters don't interpenetrate or if there are no oligomeric species to "fill-in" pores
Management of Capillary Pressure	•vary capillary pressure (P_c) to achieve desired pore size during solvent removal •$P_c = -2\gamma/r$, where γ is the surface tension and r is the pore radius	•Methods •vary ambient pressure •vary solvent composition •vary surface chemistry (changes surface tension) •go to supercritical conditions •use drying control additives (DCCAs)[9, 10]
Molecular Templating	•pore size control by the size of solvent or organic ligand to be removed	•Example: pore size increases from methanol to ethanol to isopropanol solvent
Relative rates of condensation and evaporation	•porous when condensation rate >> evaporation rate •less porous or non-porous when evaporation rate >> condensation rate	•can control relative rates of condensation and evaporation through composition, processing, aging, and drying conditions
Sintering and Surface Derivitization	•sintering to higher temperatures reduces pore volume and pore size distribution •sintering occurs by the reduction of the solid vapor interfacial energy, which can be controlled by altering the surface of the gel	

2. EXPERIMENTAL

Material Synthesis. A low molecular weight (MW=400-700) silanol-terminated polydimethylsiloxane (PDMS) (United Chemical Technologies) was the reactive polymer used to make the Polycerams. The silanol end groups of the PDMS can participate in condensation reactions with a hydrolyzed metal alkoxide or another silanol-terminated PDMS. This can result in Metal-PDMS, or PDMS-PDMS linkages, respectively. Two synthetic routes were used, Route 1 and Route 2. All the resulting samples were optically transparent and polishable.

Route 1. Tetraethoxysilane (TEOS), PDMS, ethanol (EtOH), and H_2O (acidified to 0.15 M with H_2SO_4) were refluxed in a flask for 1 hour at a EtOH:H_2O:TEOS molar ratio of 35:2:1. PDMS was added at various concentrations ranging from 0% to 80% by volume with respect to the final solid volume. A base (triethylamine or 1,4-diazobicyclo[2.2.2]octane (Dabco)) was added at base:acid mole ratio of 2:1 and the solution was mixed for 15 minutes. Pyrromethene 567 (PM-567) laser dye (synthesis reported elsewhere[11, 12]) was then added at a concentration of $5*10^{-5}$ M and the solution was concentrated. Monoliths were made by pouring the solution in polypropylene beakers and drying at 75 C for 3 days. After polishing, the resulting Polyceram disks were 2 cm in diameter and 0.4 cm thick. This synthetic route is shown schematically in Figure 1a.

Route 2. TEOS, EtOH, and H_2O (acidified to 0.15 M with H_2SO_4) were refluxed in a flask for 1 hour at a EtOH:H_2O:TEOS molar ratio of 35:3:1. A base (triethylamine or Dabco) was added at base:acid mole ratio of 2:1 and the solution was mixed for 15 minutes. PM-567 was added at $5*10^{-5}$ M, the solution was refluxed for an additional hour, and then the PDMS was added. The solutions were then concentrated and dried in polyethylene beakers with pinhole tops at 75 C for one week.

Samples were made at various PDMS contents in the solid Polyceram ranging from 0 % to 80 % by volume. This synthetic route is shown schematically in Figure 1b.

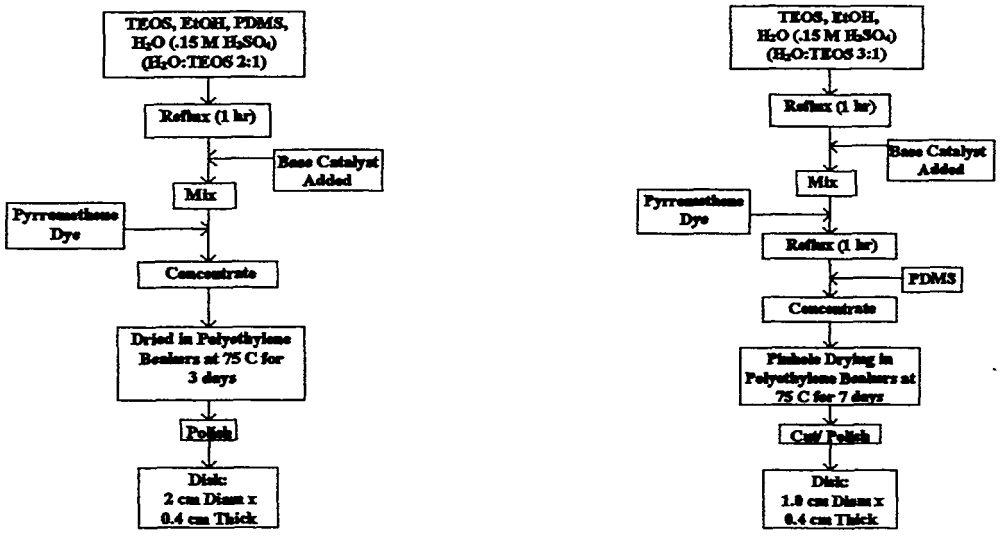

Figure 1: Schematic of SiO_2:PDMS Polyceram synthesized by (a) Route 1 and (b) Route 2.

Surface Area and Porosity Measurements. The surface area, pore volume, and pore size were determined by the N_2 (77 K) adsorption BET (Brunauer, Emmet, Teller) isotherm method[13] using a Micrometrics ASAP 2000 for the solid SiO_2:PDMS Polycerams. Typically, 0.5 gm of the solid Polyceram was degassed for 48 hours at 90 C in vacuum (10^{-6} Torr) before the adsorption measurements. All the porous samples showed Type I Isotherm behavior and fit well to the BET Isotherm. The effective cross sectional area of the N_2 cross section (which is needed to calculate the specific surface area of the material) is different for silica based materials compared with other materials[4, 14]. Ismail[14] measured silica samples with N_2 adsorption and Kr adsorption, and determined the effective cross sectional area of N_2 for silica to be 0.112 nm^2, instead of the more standard effective cross section 0.162 nm^2. The interaction of the quadrupole moment of the N_2 molecule with the hydroxyl groups on the silica surface is believed to cause the decrease in the effective cross section. The cross sectional area of N_2 determined by Ismail was used for all the porosity calculations reported here.

NMR Spectroscopy. Magic Angle Spinning (MAS) Cross Polarization (CP) ^{29}Si Nuclear Magnetic Resonance (NMR) was performed on the solid SiO_2:PDMS Polycerams using a Bruker Instruments model MSL-200. For the CP spectra, 5 ms contact time was applied, and for the MAS, a spinning rate of 3.5 kHz was used. Some samples were measured without CP in order to obtain more quantitative evaluation of the ratio of the Q species to be used in the structural model.

Density Measurements. The densities of the SiO_2:PDMS Polycerams were measured by placing the samples in a density gradient column. The gradient column was made using a 1:1 mixture of xylene (ρ=0.885 gm/cm^3) and carbon tetrachloride (ρ=1.58 gm/cm^3) within a 250 ml graduated cylinder [15]. The column was calibrated by placing polymeric pellets of known densities within the column, and the densities of the Polycerams were calculated based on the height at which the Polycerams settled in the gradient column.

3. RESULTS AND DISCUSSION

3.1 Control of Porosity as a Function of Processing

Using the BET method to evaluate the surface area and pore volume, the SiO_2:PDMS Polyceram monoliths with 40 % PDMS synthesized using Route 1 had no measurable porosity or surface area, while the monoliths with 40% PDMS

synthesized by Route 2 had a high pore fraction (0.38) and a high surface area (342 m^2/gm). These results are explained in the discussion below.

Routes 1 and 2 (Figure 1) had specific differences in their processing, which lead to changes in the relative rates of hydrolysis and condensation. First, Route 2 utilized a higher water content (H_2O:TMOS mole ratio = 3:1) compared to Route 1 (H_2O:TMOS = 2:1). This resulted in a greater degree of condensation with the Route 2 Polycerams. Second, the Route 2 solutions were refluxed for an additional hour after the base catalyst was added, while the Route 1 solutions were not refluxed after the addition of the base. This resulted in a greater condensation rate with the Route 2 Polycerams. Third, the Route 2 solutions were pin-hole dried (i.e., dried in a covered polypropylene container with pin holes to allow evaporation), while the Route 1 solutions were open-top dried (i.e., dried in an uncovered polypropylene container). This resulted in a lower evaporation rate for Route 2 solutions, allowing more time for condensation to occur than with the Route 1 solutions.

These differences in the processing between Routes 1 and 2 lead to dramatic changes in the drying behavior of the Polyceram solutions (see Figure 2). A syneresis drying behavior, where the gel network contracts and expels the liquid from the pores[2], was observed with the Route 2 Polycerams. The syneresis behavior is attributed to condensation reactions forming new bonds and causing shrinkage of the gel, thus forcing the removal of solvent. The high degree of crosslinking resulted in a high gel strength; therefore, at some point during drying, the gel gained enough strength that it did not shrink any further. Hence further solvent removal resulted in the formation of external voids or porosity within the solid sample. The drying behavior for the Route 1 Polycerams was quite different (Figure 2). Large solvent removal preceded much of the condensation reactions, because the sample did not gel until most of the solvent was removed. Sample shrinkage was governed by the evaporation; hence these samples were essentially non-porous.

The use of acid/base two-step processes allowed control of the hydrolysis/condensation reactions (Figure 3a), because the reaction kinetics were greatly dependent on the pH of the solution. The general effect of pH on the gel time for aqueous silicates is summarized in Figure 3b[16]; similar pH behavior has been observed with the hydrolysis/condensation reactions of silicon alkoxides[2]. Under acidic conditions (pH=1-3), both the hydrolysis and condensation reactions are catalyzed, but the hydrolysis rate greatly exceeds the condensation rate. This results in weakly branched structures and relatively long gel times. Under less acidic conditions (pH=3-8), the condensation rate increases and the hydrolysis rate decreases, resulting in shorter gel times. The degree of hydrolysis and condensation can then be controlled by hydrolyzing under acidic conditions and then accelerating condensation reactions by adding a base. The amount of condensation which took place in the two-step acid/base processes employed here (Routes 1 & 2) was governed by the degree of hydrolysis in the first step. For example, under partial hydrolysis conditions, all the alkoxide groups were not hydrolyzed after the first step. Upon addition of the base, the condensation rate is enhanced. However, the water-producing condensation rate is greater than the alcohol producing condensation rate[2] (see Figure 3a). Hence the degree of condensation is largely limited to the number of hydrolyzed species.

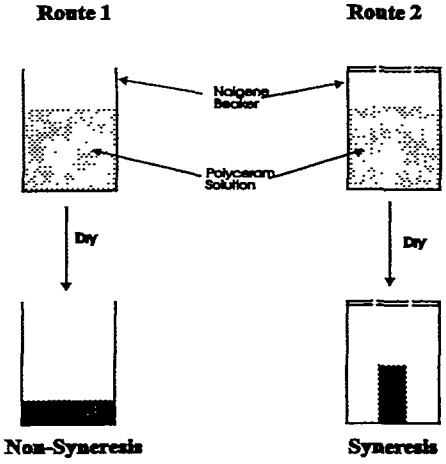

Figure 2: Differences in drying behavior of the SiO_2:PDMS Polyceram solutions processed using Routes 1 and 2.

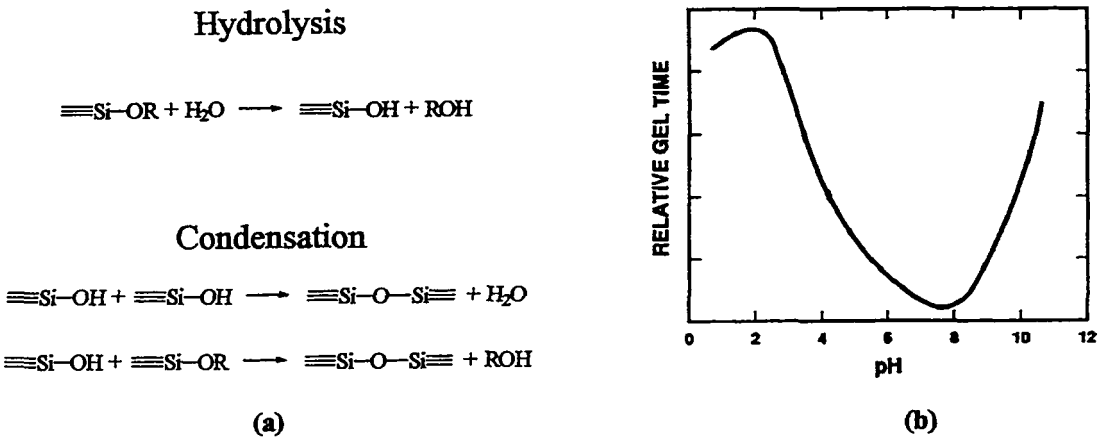

Figure 3: (a) Schematic of hydrolysis and condensation reactions and (b) gel time as a function of pH for aqueous silicates. After Iler[16].

Solid-state ^{29}Si NMR is a useful technique for examining the structure of silicates [17-21]. A variety of silicate structures can be formed in the sol-gel process and they can be described by three major silicate species: (1) Q species which represents a quartenary oxygen tetrahedron; (2) T species which represents a three oxygen, one alkyl group tetrahedron; and (3) D species which represents a two oxygen, two alkyl group tetrahedron. Superscripts after the Q, T, or D nomenclature denote the number of alkoxide groups which have reacted to form Si-O-Si linkages. Therefore, Q^0, T^0, and D^0 represent unreacted precursors, while Q^4, T^3, and D^2 represent completely reacted species. In this study, Q species signify Si-O species from TEOS, and D species signify Si-O species from PDMS. There are no T species in the present Polycerams. CP and MAS techniques were used to obtain enhanced signals and resolution with solid-state ^{29}Si NMR spectra. This technique was applied to determine the degree of silica and PDMS crosslinking within the Route 1 and Route 2 Polycerams. The CP-MAS ^{29}Si NMR spectra for all of the SiO_2:PDMS Polycerams used in this study are shown in Figure 4. Comparison of the NMR spectra for SiO_2:PDMS Polycerams (40 volume % PDMS) synthesized by Routes 1 and 2 shows that the silica species are more crosslinked in the Route 2 Polyceram; the Route 2 Polyceram has less Q^1 and Q^2 species compared to the corresponding Route 1 Polyceram. This confirms the high degree of condensation of the Route 2 Polycerams with respect to the Route 1 Polycerams and supports our hypothesis of porosity control.

The interpretation of the crosslinking of the PDMS (D species) is more complex. D^2 and D^1 peak assignments have been previously reported with values of -19 to -23 and -12 ppm, respectively[17, 22, 23]. The PDMS oligomer contains approximately seven Si atoms. That means that five of the Si atoms have a D-D^2-D character, while the two Si atoms at the ends of the PDMS can have different types of bonding. In our system it is not possible to obtain the D^0 peak at -4.8 ppm[22, 23] because that could only occur if the monomer of PDMS was present in the system; only D^1 and D^2 peaks are possible. The amount of D^1 (-12 ppm) present was very small (<5%) in both 40% PDMS Polycerams (Figure 4), suggesting that most of the PDMS have condensed. A sharp D^2 peak at -23.5 ppm was observed with both samples, which represents both the Si atoms within the PDMS oligomer and the Si atoms connected to the silanol groups at the ends of the oligomer which have condensed to another PDMS (D-D^2-D).

Both samples also had an additional broad D^2 peak (referred to as D^{2*}) with chemical shifts between -18 to -21 ppm (Figure 4). The broad peak stems from the use of the CP technique, which enhances the intensity of Si atoms located near H atoms (<10 Å)[24]. The broad peak corresponds to D^{2*} units in more constrained environments. In other words, it represents D^2 species bonded to various Q species or D species trapped around a Q skeleton. This has been argued from the much longer CP relaxation time for the sharp D^2 peak (6.0 msec) compared to that of the broad D^{2*} peak (0.8 msec)[23]. In other silicate materials, CP relaxation times have been observed to decrease when the species are locally constrained. Broad

D^{2*} peaks have also been identified with CP-MAS ^{29}Si NMR spectra of other PDMS/TEOS systems as well as in (dimethyldiethoxysilane) DEDMS / TEOS and DEDMS / (titanium tetraisopropoxide) TIP nanocomposites[23, 25].

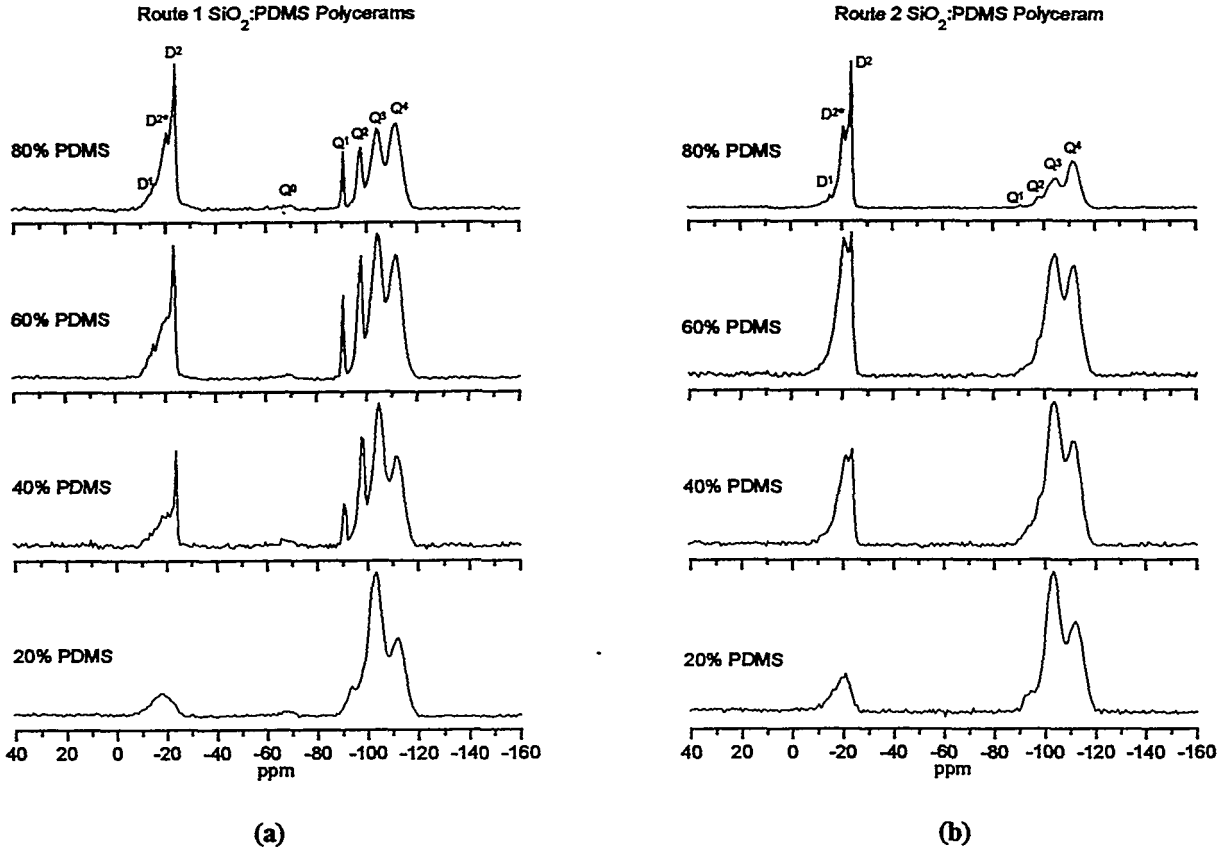

Figure 4: CP-MAS ^{29}Si NMR spectra for SiO_2:PDMS Polycerams with varying PDMS contents synthesized by (a) Route 1 and (b) Route 2.

The Route 2 Polyceram had a narrower co-condensation peak (D^{2*}) than the Route 1 Polyceram. The Route 1 Polyceram is more likely to have various D^2 species condensing with various Q species (D^2-Q^1, D^2-Q^2, D^2-Q^3, D^2-Q^4), while the D^2 species in the Route 2 Polycerams is more limited to co-condensation with Q^3 and Q^4 species (D^2-Q^3, D^2-Q^4) because there are few Q^1 and Q^2 species. Overall, the D^{2*} peak signifies that a large degree of co-condensation is occurring between the D and Q species, suggesting that organic and inorganic species are mixing close to the molecular level. The differences between the two Polycerams (Routes 1 and 2) is in the degree of crosslinking and the porosity.

3.2 Control of Porosity as a Function of Composition

Not only was the porosity controlled by variations in the synthetic route, but also by the PDMS content. Table 2 summarizes the properties of SiO_2:PDMS Polycerams synthesized by Routes 1 and 2 having various polymer contents. Figure 5a is a plot of the surface area of SiO_2:PDMS Polycerams synthesized by Routes 1 and 2 as a function of polymer content. The surface area of the 0 volume % PDMS sample synthesized by Route 2 was high at 573 m^2/gm. As the polymer content increased, the surface area and the porosity decreased, and reached zero at 60 volume % PDMS (Figure 5a). The pore size stayed essentially constant at about 40 Å. In contrast, the Route 1 Polycerams were all non-porous regardless of the polymer content.

The term 'non-porous' used in the present study represents a solid which is impermeable to N_2 molecules at 77K. That does not mean that these Polycerams are completely non-porous. First, the Polycerams may contain internal porosity which adsorption techniques cannot measure. Second, N_2 adsorption techniques cannot measure micropores (7 to 15 Å) and

submicropores (< 7 Å), because these micropores are often not accessible to small molecules, such as N_2, at low temperatures[4, 14]. Regardless of the faults of the quantitative nature of the N_2 adsorption measurements, the results demostrate that porosity can be varied dramatically with change in polymer content and processing route.

Table 2: Properties of SiO_2:PDMS Polycerams at various PDMS contents synthesized by Route 1 and Route 2.

Sample	Physical Properties	BET Surface Area (m^2/g)	Pore Size	Density (gm/cm^3)	Pore Volume (Volume Fraction pores)
Route 1 20% PDMS	non-syneresis drying, water resistant, hard	0.91	—	1.49 ±.01	0.00 (0.00)
Route 1 40% PDMS	non-syneresis drying, water resistant, hard	0.00	—	1.37 ±.01	0.00 (0.00)
Route 1 60% PDMS	non-syneresis drying, slow gelling, hard	0.00	—	1.31 ±.01	—
Route 1 80% PDMS	non-syneresis drying, slow gelling, soft	—	—	1.197	—
Route 2 0% PDMS	syneresis drying, brittle, very H_2O sensitive	573	42 Å	1.35 ±.01	0.59 cm^3/gm (0.79)
Route 2 20% PDMS	syneresis drying, brittle, H_2O sensitive	513	42 Å	1.124 ±.01	0.53 cm^3/gm (0.59)
Route 2 40% PDMS	syneresis drying, least tendency to crack, hard	342	39 Å	1.168 ±.01	0.33 cm^3/gm (0.38)
Route 2 60% PDMS	syneresis drying, hard	0.27	—	1.25 ±.01	0.001cm^3/gm (0.00)
Route 2 80% PDMS	less syneresis drying	—	—	1.22 ±.01	—

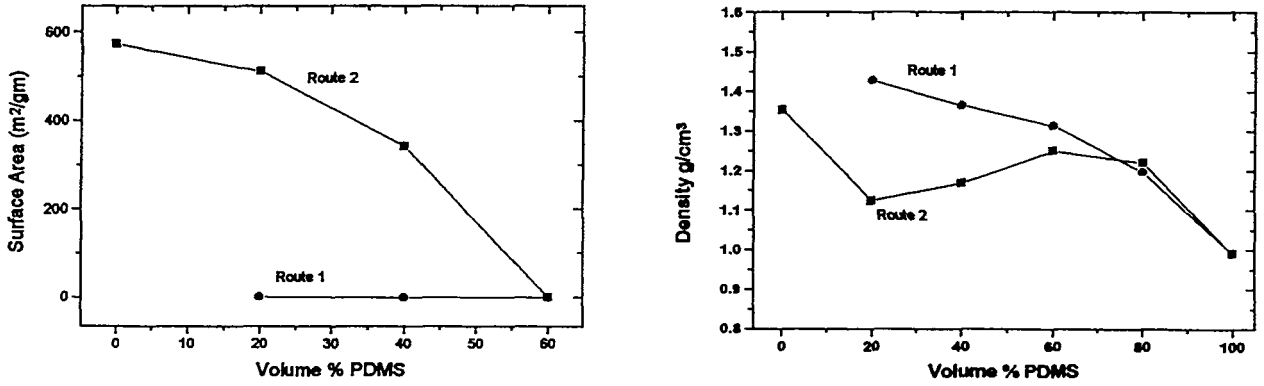

(a) (b)

Figure 5: (a) Surface area and (b) density of SiO_2:PDMS Polycerams synthesized by Routes 1 and 2 as function of the PDMS content.

The effect of polymer content on porosity and drying behavior with the Route 2 Polycerams can be associated with two phenomena: (1) the polymer "fills-in" the pores as the polymer content increases, thereby reducing the porosity; and (2) the silica condensation decreases as the polymer content increases due to co-condensation and steric hindrance. These phenomena are examined in the following discussion.

A more detailed look at the drying behavior of the Polycerams provides insights into possible structural changes as a function of polymer content. Two basic types of drying behavior were observed; syneresis and non-syneresis (Figure 2). For syneresis drying to occur, one would expect the continuous matrix to be largely SiO_2 and not PDMS. In the range of 0-60% PDMS, syneresis drying behavior was observed with the Route 2 Polycerams but not with the Route 1 Polycerams. The Route 2 Polyceram at 60% PDMS was, however, also non-porous. If the reduction in porosity was caused solely by a decrease in the condensation, one would expect non-syneresis drying behavior with this sample. Instead, identical syneresis behavior (i.e., same radial shrinkage ($\Delta r/r$)) was observed with these Polycerams. The polypropylene beaker in which the Polyceram solutions were dried had a diameter of 2.2 cm, while the final monolith in the polymer content range of 0-60 % PDMS had a diameter of 1.0 cm. The height of these samples varied slightly, corresponding to measured densities of these samples. Because these samples shrank the same amount in the radial direction, this suggests that in the range of 0-60% PDMS the degree of silica condensation did not decrease dramatically and that the PDMS served effectively to "fill-in" the pores of the host matrix.

The "fill-in" idea would suggest that the inorganic framework is forming independently of the PDMS. However evaluation of the CP-MAS ^{29}Si data in Figure 4 gives strong evidence that there is a large amount of PDMS co-condensation and PDMS in Q environments due to the presence of the D^{2*} peak. The co-condensation of the PDMS could occur at the silica pore surface which would coincide with the "fill-in" model. The calculated pore volume required to "fill-up" all the silica pore surface in the 0% PDMS Route 2 Polyceram (surface area=573 m^2/gm), assuming the PDMS co-condenses to the silica pore surface at a cross-sectional area of 16 $Å^2$, is approximately 50-60 volume % PDMS. This back-of-the-envelope calculation corresponds well to observed surface area measurements in which the Polyceram becomes non-porous at 60% PDMS (Figure 5a), suggesting that it is possible for all the PDMS to co-condense at the silica pore surface. On the other hand, the co-condensation of PDMS could also result in the PDMS becoming a part of the continuous silica matrix, which would contribute to the decrease in the Q condensation due to steric hindrance of the PDMS. However for syneresis drying behavior to occur, it is likely that the continuous matrix is mostly inorganic with some co-condensation occurring within the inorganic framework, while most of the co-condensation occurs at the pore surface.

Further evidence supporting that PDMS is "filling-up" the pores as well as incorporating in the continuous silica matrix is suggested by the NMR Data (Figure 4b). At low PDMS contents (20% PDMS), the sharp D^2 peak is not observed, suggesting that almost all the PDMS oligomers are constrained in a silica environment (i.e., all the PDMS is in the continuous silica matrix and/or co-condensed at the pore surface). As the polymer content increased, the sharp D^2 peak becomes more pronounced. Hence more PDMS is occupying PDMS-rich regions or voids of the structure instead of occupying parts of the continuous silica matrix. At very high Polymer contents (80% PDMS), Q condensation appears to be significantly reduced. This is especially seen with the CP-MAS ^{29}Si NMR data with a significant increase in the Q^1 and Q^2 species relative to the Q^3 and Q^4 species of the Route 2 Polycerams from 60% PDMS to 80% PDMS (Figure 4b). Since the PDMS has occupied all the pores at 60% PDMS, further increase in the PDMS content disrupts more of the continuous silica matrix. Less syneresis drying (reflected by less shrinkage across the diameter and greater shrinkage across the height) of the 80% PDMS Polyceram (Route 2) compared to its 60% PDMS counterpart also supports this.

The location of the PDMS in the final structure is likely governed by competition of thermodynamic and kinetic driving forces. The driving force for the PDMS to go to the pores of the silica matrix may stem from large differences in the solubility parameters of PDMS (δ=8.16 $(cal/cm^3)^{1/2}$) and the silica surface (δ =13.39 $(cal/cm^3)^{1/2}$). The solubility parameters were calculated by summing up the group contributions of the cohesive energies and molar volumes[26]. The silica surface was represented by a partially reacted TEOS, where Si is bonded to one ethoxide group and one hydroxyl group. On the other hand, the PDMS is kinetically driven to be located in the continuous silica matrix due to the co-condensation reactions between the silica and PDMS.

If PDMS "fills-up" the pores of the matrix, then the size of the phase separation between the PDMS and silica matrix should be equivalent to the pore size. The pore size was small, ≈40 Å; therefore, the size of the phase separation should be ≈40 Å. For size comparison, the pore size is about the stretched length of only 3-4 PDMS oligomers.

The effect of PDMS content on the structure of the Route 1 Polycerams was different. Since the overall degree of condensation was low, the syneresis drying behavior did not occur and the materials were non-porous for all polymer contents. The PDMS cannot be drawn to the pores as in the Route 2 Polycerams. Therefore, it is believed that the PDMS

addition to the Polyceram causes a more steric hindrance effect on the Q condensation. In Figure 4a, the Q^1 and Q^2 species increase noticeably with increase in PDMS content, reflecting the decrease in the Q condensation.

The densities of the Polycerams as a function of PDMS content and processing route shown in Figure 5b correlate well with the porosity measurements. The density of the Polycerams (ρ_t) can be described as:

$$\rho_t = V_{SiO2}\,\rho_{SiO2} + V_{PDMS}\,\rho_{PDMS} + V_{pore}\,\rho_{pore}$$

where ρ_{SiO2} is the skeletal density of the silica matrix, ρ_{PDMS} is the density of the PDMS polymer, ρ_{pore} is the density of the pore, V_{SiO2} is the volume fraction silica, V_{PDMS} is the volume fraction PDMS, and V_{pore} is the pore volume. The density of the polymer is 0.991 gm/cm^3 and the density of the air is 0.001 gm/cm^3. The theoretical skeletal density of silica has been reported as 2.05 gm/cm^3, although reported values for the skeletal density tend to vary depending on processing conditions (ranging from 1.88 to 2.19 gm/cm^3)[2]. Since all the Route 1 Polycerams were non-porous, the density decreased with increase in PDMS content because the density of PDMS is much less than the silica skeletal density. The Route 2 Polycerams were porous at PDMS contents less than 60%, and increases in the PDMS content up to 60% resulted in an increase in density, likely reflecting a "filling-up" of the voids in the structure. At higher PDMS contents (>60%), the Polycerams are non-porous, and the density decreases with increasing PDMS content (just as with the Route 1 Polycerams).

3.3 Structural Model and Photostability Case Study

The BET and NMR data on the SiO_2:PDMS Polycerams were used to produce 2D structural models to illustrate the concepts generated in the present study. These structural models are utilized as a case study for the specific application of laser dyes incorporated within Polyceram hosts. In previous studies performed in our laboratory, we doped a Pyrromethene laser dye within SiO_2:PDMS Polycerams to examine how the porosity and composition affect the photostability of the laser dyes[11, 12, 27]. The results indicated that photostability improved with decreasing porosity and increasing silica content. These photostability results on the Routes 1 and 2 Polycerams are correlated with the structural model.

The CP-MAS ^{29}Si NMR data in Figure 4 could not be used quantitatively to describe the ratio of the Q species. Because the cross polarization technique was used, there is an enhanced signal from silicate species located near hydrogen atoms. This allowed for investigation of the PDMS located in a constrained environment, but eliminated the possibility of evaluating the Q species quantitatively. Low Q species, such as Q^0, Q^1, and Q^2, had an enhanced response with respect to higher Q species (Q^3,Q^4), because the low Q species are more likely to have hydrogen atoms located near them. For this reason, the MAS ^{29}Si NMR measurements for some of the Polycerams were repeated without CP. The determined chemical shifts and the fraction of D or Q species are illustrated in Table 3.

Table 3: Chemical shifts ppm for SiO_2:PDMS Polycerams measured by MAS ^{29}Si NMR (No CP). Values in parentheses represent the fraction of Q^x species with respect to total amount of Q species present in the sample.

Sample	Q^0	Q^1	Q^2	Q^3	Q^4	Q^1:Q^2:Q^3:Q^4
20% PDMS Route 1	-67.3 (<.01)	-93.9 (.07)	-98 (.07)	-103.0 (.44)	-111.7 (.43)	1.0:1.0:6.3:6.1
40% PDMS Route 1	-67. (<.01)	-90.5 (.07)	-97.6 (.18)	-104.2 (.37)	-111.6 (.38)	1.0:2.6:5.3:5.4
20% PDMS Route 2	— (.00)	≈-92 (.04)	≈-98 (.03)	-103.2 (.42)	-111.6 (.51)	1.0:0.8:10.5:12.8
40% PDMS Route 2	— (.00)	-92.9 (.03)	-97.8 (.04)	-103.9 (.45)	-111.5 (.48)	1:1.3:15.0:16.0

In the proposed model, TEOS is represented by a "+" where the four ends correspond to the four functionality of TEOS, and the PDMS is represented by a thick curly line. The sizes of the species present in the Polycerams have been taken into account (1.2 Å for an O_2 molecule,1.6 Å for a Si-O-Si bond, 8-10 Å x 4 Å for a PDMS oligomer, and 13 Å x 6.4 Å for the PM-567 dye molecule). The dye concentration within a Polyceram is $5*10^{-5}$ M corresponding to $6*10^{17}$ cm^{-3} and an average dye-dye distance of about 120 Å. The oxygen concentration within PDMS will be used for the lack of a better value for the Polycerams, corresponding to $4.7*10^{18}$ cm^{-3} [28]. This results in an O_2:dye ratio of approximately 8:1. The oxygen molecules were randomly distributed in the structure, although there is a tendency for the O_2 molecules to be located

at the pore surface[29, 30]. From the BET data, the average pore size and pore fraction were utilized (Table 2). For example, the 40% PDMS Polyceram synthesized by Route 2 has an average pore size of 42 Å and a open pore fraction of 0.38. It is assumed that the Polyceram also has microporosity and some closed porosity. Also, from the MAS ^{29}Si NMR data, the ratio of Q^1:Q^2:Q^3:Q^4 (Table 3) gives guidelines for connecting the "+" species to each other. The degree of PDMS condensation is high, based on the presence of the co-condensation D^2* NMR peak in Figure 4. For the 40% PDMS Polycerams the SiO_2:PDMS ratio is 26:1 and for the 20% PDMS Polycerams the ratio is 76:1. Taking all these factors into account for each of the compositions described in Table 3, proposed structures for the SiO_2:PDMS Polycerams are shown in Figure 6.

The structural model illustrates a number of concepts discussed earlier in this paper. First, the Route 1 Polycerams are less condensed as seen by the greater number of Q^1 and Q^2 species (Figure 6a and 6c) compared to the Route 2 Polyceram (Figure 6b and 6d). Second, the Route 1 Polycerams do not have any external porosity, but do contain some microporosity and closed pores. Third, the porous nature of the material and the reduction in porosity with increase in polymer content of the Route 2 Polycerams are seen in the structural models. Finally, the structural models also illustrates how it is possible to have polymer co-condensed in the continuous silica matrix as well as have the remaining polymer 'filling-up" the small pores in the matrix. The ratios of the Q species define a set of boundary conditions on the structural model and imposes constraints on the structure of the silica matrix.

The structural model also helps illustrate why the photostability of the dye doped Polycerams is improved in non-porous and high silica Polycerams. It was determined in previous investigations that the Pyrromethene dye molecules degrades upon exposure to light by oxidation processes[12, 27]. Therefore the ability of oxygen to arrive at the dye molecules should determine whether the dye will react with oxygen. The model illustrates the large presence of oxygen in the Polyceram with respect to the dye and its easy access to the dye molecules located in the pores of the porous Polycerams (Figures 6b and 6d). The size of oxygen with respect to the pores is very small, and the diffusion of oxygen through the pores is likely very high. The structures for the 20% and 40% PDMS Polycerams synthesized by Route 1 (Figures 6a and 6c) portray a more difficult access of oxygen to the dye because of the non-porous nature of the material. In addition, the structure shows that the pores have varying degrees of accessibility for oxygen. The more porous the host material, the easier it is for oxygen to interact with the dye and undergo photochemical reaction to cause photodegradation. Photostability also improved with increasing SiO_2 content. The greater the SiO_2 content, the greater the chance of the dye to be caged due to the greater functionality of the SiO_2 (4 functional) compared to PDMS (2 functional). The improved photostability of the higher SiO_2 Polycerams also stems from the lower diffusivity of O_2 through dense SiO_2 versus PDMS[12, 28, 31, 32]. There is likely a distribution of dye molecules located within the pores and cages of the matrix, each dye molecule having a different probability of reacting with an oxygen molecule in a given time[12, 27].

CONCLUSIONS

Using two step acid/base sol-gel processes, a variety of optically transparent sol-gel monoliths have been synthesized. The control of the relative rates of condensation and evaporation as well as the polymer content made it possible to control the amount of porosity within the SiO_2:PDMS Polycerams ranging from materials with very high surface areas to materials which are essentially non-porous. These materials represent a new class of engineered porous materials. A structural model based on porosity measurements and ^{29}Si NMR data, correlates proposed structures to the physical properties and photostability characteristics of these materials.

ACKNOWLEDGEMENTS

The financial support of the Air Force Office of Scientific Research, the Corning Foundation Fellowship, and the Chapman Fellowship are gratefully acknowledged. The services of Kenner Christensen in performing the ^{29}Si NMR experiments is also acknowledged.

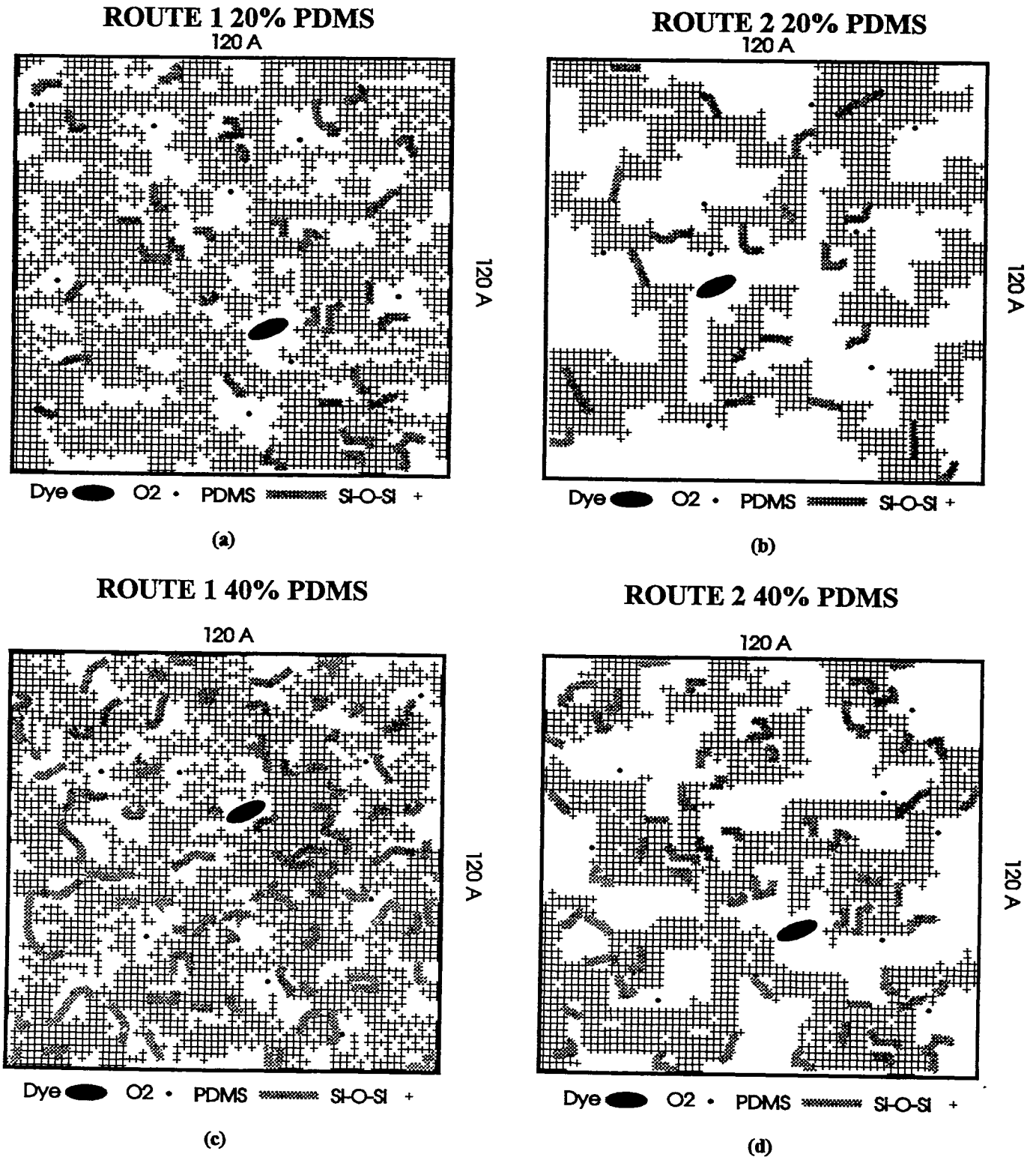

Figure 6: Proposed structures of SiO_2:PDMS Polycerams (a) at 20 vol % PDMS (Route 1), (b) at 20 vol % PDMS (Route 2), (c) at 40 vol % PDMS (Route 1), and (d) at 40 vol % PDMS (Route 2).

REFERENCES

1. D. W. Schaefer, *MRS Bulletin* **XIX**, 14-17 (1994).
2. C. Brinker, G. Scherer, *Sol-Gel Science* (Academic Press, Inc., Boston, 1990).
3. C. Brinker, S. Wallace, N. Raman, R. Sehgal, J. Samuel, S. Contakes, in *Access in Nanoporous Materials* T. Pinnavaia, M. Thorpe, Eds. (Plenum Press, New York, 1995) pp. 123-139.
4. F. Ehrburger-Dolle, J. Dallamano, G. Pajonk, E. Elaloui, in *Characterization of Porous Solids III* (1994), vol. 87, pp. 715-724.
5. L. Balducci, F. Montino, G. Cogliati, US Patent 5,270,027 (Istituto Guido Donegani, 1993).
6. M. McClain, D. Loy, S. Prabakar, in *Better Ceramics Through Chemistry VII: Organic/Inorganic Hybrid Materials* (MRS, 1996), vol. 435, pp. 277-282.
7. C. Guizard, P. Heckenbenner, J. Schrotter, N. Hovnanian, M. Smaihi, in *Better Ceramics Through Chemistry VII: Organic/Inorganic Hybrid Materials* . (MRS, 1996), vol. 435, pp. 283-294.
8. S. Kramer, F. Rubio-Alonso, J. D. Mackenzie, in *Better Ceramics Through Chemistry VII: Organic/Inorganic Hybrid Materials* (MRS, 1996), vol. 435, pp. 295-300.
9. L. Hench, in *Science of Ceramic Chemical Processing* D. R. Ulrich, L. Hench, Eds. (Wiley, New York, 1984) pp. 52.
10. S. Wallace, L. Hench, *Mat. Res. Soc. Symp. Proc.* **32**, 47 (1984).
11. T. Suratwala, Z. Gardlund, K. Davidson, D. R. Uhlmann, S. Bonilla, N. Peyghambarian, *Journal of Sol-Gel Science and Technology* **8**, 953-958 (1997).
12. T. Suratwala, Ph.D. Dissertation, University of Arizona (1996).
13. S. Lowell, *Introduction to Powder Surface Area* (John Wiley & Sons, New York, 1979).
14. I. Ismail, *Langmuir* **8**, 360-365 (1992).
15. C. Stock, E. Scofield, *Textile Research Journal* **July**, 521-526 (1951).
16. R. Iler, *The Chemistry of Silica* (John Wiley & Sons, New York, 1979).
17. R. Glaser, G. Wilkes, C. Bronnimann, *Journal of Non-Crystalline Solids* **113**, 73-87 (1989).
18. E. Lippmaa, M. Magi, A. Samoson, G. Engelhardt, A. Grimmer, *J. Am. Chem. Soc.* **102**, 4889 (1980).
19. G. Engelhardt, H. Jancke, E. Lippmaa, A. Samoson, *J. Organometallic Chem.* **210**, 295 (1981).
20. M. Magi, E. Lippmaa, A. Somoson, G. Engelhardt, A. Grimmer, *J. Phys. Chem.* **88**, 1518 (1984).
21. J. Kim, J. Plawsky, E. Wagenen, G. Korenowski, *Chem. Mater.* **5**, 1118-1125 (1993).
22. F. Babonneau, *New J. Chem.* **18**, 1065-1071 (1993).
23. F. Babonneau, *Mat. Res. Soc. Symp. Proc.* **346**, 949-960 (1994).
24. W. Klemperer, V. Mainz, D. Millar, *Mat. Res. Soc. Symp. Vol.* **73**, 15-25 (1986).
25. F. Babonneau, L. Bois, J. Livage, S. Dire, in *Nanophase and Nanocomposite Materials* S. Komarneni, J. Parker, G. Thomas, Eds. (MRS Symposium Proceedings, 1993), vol. 286, pp. 289-294.
26. D. W. VanKrevelen, *Properties of Polymers: Their Estimation and Correlation with Chemical Structure* (Elesevier Scientific Publishing Company, Amsterdam, 1976).
27. T. Suratwala, K. Davidson, Z. Gardlund, D. R. Uhlmann, S. Bonilla, N. Peyghambarian, *Solid State Lasers VI* **SPIE 2986**, 141-152 (1997).
28. B. Arkles, *Gelest Product Catalog* (1995).
29. A. Levy, D. Avnir, *J. Phys. Chem.* **97**, 10380-10384 (1993).
30. J. Samuel, M. Ottolenghi, D. Avnir, *Physica A* **191**, 153-167 (1992).
31. S. Pauly, in *Polymer Handbook* J. Brandrup, E. Immergut, Eds. (John Wiley & Sons, New York, 1989), vol. VI, pp. 435-449.
32. W. Kingery, H. Bowen, D. R. Uhlmann, *Introduction to Ceramics Second Edition* (John Wiley & Sons, New York, 1976).